PRAMANA — journal of physics
© Indian Academy of Sciences
Vol. 79, No. 1
July 2012
pp. 137–150

The relationship between the doping levels and some physical properties of SnO_2:F thin films spray-deposited on optical glass

DEMET TATAR* and BAHATTIN DÜZGÜN

K.K. Education Faculty, Department of Physics, Ataturk University, Erzurum 25240, Turkey
*Corresponding author. E-mail: demettatar@atauni.edu.tr

MS received 24 October 2011; revised 9 January 2012; accepted 23 January 2012

Abstract. The relationship between the fluorine doping level and the electrical, structural and optical properties of the SnO_2:F films are investigated using the Hall effect measurement set-up in van der Pauw configuration, the XRD patterns, UV–vis spectrophotometry and atomic force microscopy (AFM). The X-ray diffraction patterns taken at room temperature show that the films are polycrystalline. The preferred directions of crystal growth in the diffractogram of SnO_2:F (FTO) films correspond to the reflections from the (1 1 0), (2 0 0), (2 1 1) and (3 0 1) planes. Thin film thickness and the grain size vary from 280 to 1545 nm and from 17.45 to 33.22 nm, respectively. AFM study reveals the surface of FTO to be made of nanocrystalline particles. The electrical study reveals that the films are degenerate and exhibit n-type electrical conductivity. The FTO films have a minimum resistivity of 5.29×10^{-4} Ω·cm, carrier density of 0.09×10^{20} cm^{-3} and mobility of 377.02 $cm^2/V{\cdot}s$. The sprayed FTO film has the minimum sheet resistance of 5.69 Ω/cm^2 and the highest figure-of-merit of 204×10^{-4} Ω^{-1} at 700 nm. The resistivity attained for the doped film in this study is lower than the values reported for 20 wt.% fluorine-doped tin oxide films prepared from the aqueous solution of $SnCl_2{\cdot}2H_2O$ precursor. The highest visible transmittance (700 nm) of the deposited films is 91.8% for 25 wt.% fluorine-doped tin oxide films. The obtained results reveal that the structures and properties of the films are greatly affected by doping levels. These films are useful as conducting layers in electrochromic and photovoltaic devices.

Keywords. SnO_2:F; optoelectronic; spray pyrolysis; thin films.

PACS Nos 73; 73.20.At; 78.15.+e

1. Introduction

The highly transparent and conducting thin films, owing to its high transmittance and conductivity, have wide applications [1,2]. In recent years, there has been a growing interest in the use of transparent conducting oxide thin films as conducting solar window materials in thin film solar cells [3–6], as heat reflectors for advanced glazing in solar application

[7,8] and as gas sensors [5–13]. Tin oxide is the first transparent conductor which is significantly commercialized [5,9,14]. Among the different transparent conductive oxides, SnO_2 films doped with fluorine or antimony seem to be the most appropriate for use in solar cells, owing to its low electrical resistivity and high optical transmittance. SnO_2 is chemically inert, mechanically hard, and can resist high temperatures [5]. Many excellent reviews of transparent conductive oxides are available [15]. Doped or undoped SnO_2 can be synthesized by numerous techniques such as thermal evaporation [3,9], sputtering [5,9–12,16,17], chemical vapour deposition [3,18–20], sol–gel dip coating [3,17,21], painting [3,17,22], spray pyrolysis [3,5,7,13,20,23–26], hydrothermal method [27] and pyrosol deposition [3,20,28–30]. Among the various deposition techniques, the spray pyrolysis is the most suitable method for the preparation of doped tin oxide thin films because of its simple and inexpensive experimental arrangement, ease of adding various doping materials, reproducibility, high growth rate and mass production capability for uniform large area coatings, which are desirable for industrial solar cell applications [3,5,11,13,17,23,31,32]. However, large area film production is economical and this is the essential characteristic of the simple spray pyrolysis technique [16]. Usually, the chemical spray pyrolysis route is used to deposit FTOs at optimized substrate temperatures of around 723–748 K [20]. Tin oxide is a wide band gap ($\sim$4 eV) and indirect band gap (of about 2.6 eV) nonstoichiometric semiconductor [33,34]. It has low n-type resistivity ($10^{-3}\ \Omega$ cm) and high transparency (90%) in the visible region [35].

In the present work, SnO_2:F thin films were prepared by the spray pyrolysis (SP) technique at substrate temperature of 440 °C using dehydrate stannous chloride ($SnCl_2{\cdot}2H_2O$) (98% purity, Merck) and ammonium fluoride (NH_4F) (99% purity, Merck) as precursors. The aim of this work is to study the relationship between the doping levels and some physical properties of SnO_2:F thin films such as the electrical, structural and optical properties. The results obtained are compared and discussed with the specified results by several researchers.

2. Experimental details

The fluorine-doped tin oxide thin films in the present study were prepared using a homemade spray pyrolysis apparatus. Thin films of SnO_2:F (FTO) were deposited on an optical glass substrate ($75 \times 25 \times 1$ mm^3). Dehydrate stannous chloride ($SnCl_2{\cdot}2H_2O$) (98% purity Merck) was used for making the precursor solution for SnO_2 thin films. 10 g of $SnCl_2{\cdot}2H_2O$ dissolved in 5 ml of concentrated hydrochloric acid (HCl) was heated at 90°C for 10 min. HCl was added to break down the polymer molecules that were formed when diluting with methanol. This mixture diluted by adding methanol served as starting solution and the diluted solution was made up to 25 ml. For fluorine doping, ammonium fluoride (NH_4F) (99% purity, Merck) dissolved in doubly distilled water (25 ml) was added to the starting solution, so that fluorine doping was in the range of 10–35 wt.%, at an interval of 5 wt.%. In each case, the spray solutions prepared was 50 ml. The spray solutions were magnetically stirred for 1 h and finally were filtered by a syringe filter having 0.2 μm pore size before spraying on the substrate. Microscopic glasses having $75 \times 25 \times 1$ mm^3 dimension were used as substrates. The substrates were washed with water, then boiled in concentrated chromic acid and kept in distilled water for 48 h [4];

finally substrates were cleaned with organic solvents and ultrasonic cleaner. The substrates were pre-heated to the required temperature. The normalized distance between the spray nozzle and the substrate was 40 cm and the spray angle (α) was 45°. The flow rate (1.25 ml/min), total spraying quantity (50 ml) and plate rotation speed (20 rpm/min) were kept fixed. Filtered compressed air was used as the carrier gas. The flow rate of air used as a carrier gas was about 1.25 ml/min. The total deposition time was maintained at 40 min for each film. The substrate temperature (working temperature) was 440°C. The substrate temperature was maintained using a k-type thermocouple-based digital temperature controller. Uniform coating was achieved by rotating the substrate with a speed of 20 rpm/min in its plane. The samples were produced simultaneously at a substrate temperature of 440°C. After deposition, the coated substrates were allowed to cool down naturally to room temperature. In each process, more samples were produced simultaneously at each doping levels. It was realized that the crystals have similar properties and then investigated some physical properties.

The structural characterization of the films was carried out by X-ray diffraction (XRD) measurements using a Rigaku D/Max-IIIC diffractometer with CuKα radiation (λ = 1.5418 Å), at 30 kV, 10 mA. Film thicknesses were measured by a conventional mass method and were confirmed with the Swanepoel method [30,36]. Surface morphology of the resulting films was examined using atomic force microscopy (AFM) (Nanomagnetics-Instrument). The electrical measurements were carried out by Hall measurements in Van der Pauw configuration at room temperature. Optical transmittance measurements of the FTO films were carried out using UV–vis spectrophotometer (Perkin–Elmer, Lambda 35) in wavelength ranging from 300 to 1000 nm.

3. Results and discussion

3.1 *Structural properties*

The surface morphology of the films was studied by AFM. The AFM surface 2D images obtained for SnO_2:F films prepared with different fluorine doping concentrations are shown in figure 1. Smaller grains started appearing on the surface, once the fluorine doping has commenced. The root mean square (RMS) values of surface roughness is found to be 30–202 nm in FTO films. The RMS roughness of the films doped with 20 wt.% F is the lowest in comparison with other films (table 1). Figure 1 shows 2D AFM images from 10 wt.% to 35 wt.% F-doped SnO_2 films. Detailed AFM study reveals that the roughness of the film depends on the doping levels. From AFM images, it was observed that the grain size become larger and the crystallinity was improved with the increase in doping levels.

The XRD patterns recorded for SnO_2:F thin films deposited by the spray pyrolysis technique as a function of the doped levels are shown in figure 2. The films are polycrystalline and two directions of crystal growth appear in the diffractogram of the film deposited at the lower doping concentration, corresponding to the reflections from the (2 0 0) and (3 0 1) planes. With the increase in the doping concentration, a new direction of crystal growth appears, corresponding to the reflection from the (1 1 0), (2 1 1) and (2 0 0) planes. The presence of other peaks such as (1 0 1), (2 2 0), (3 1 0), (3 0 1), (3 2 1)

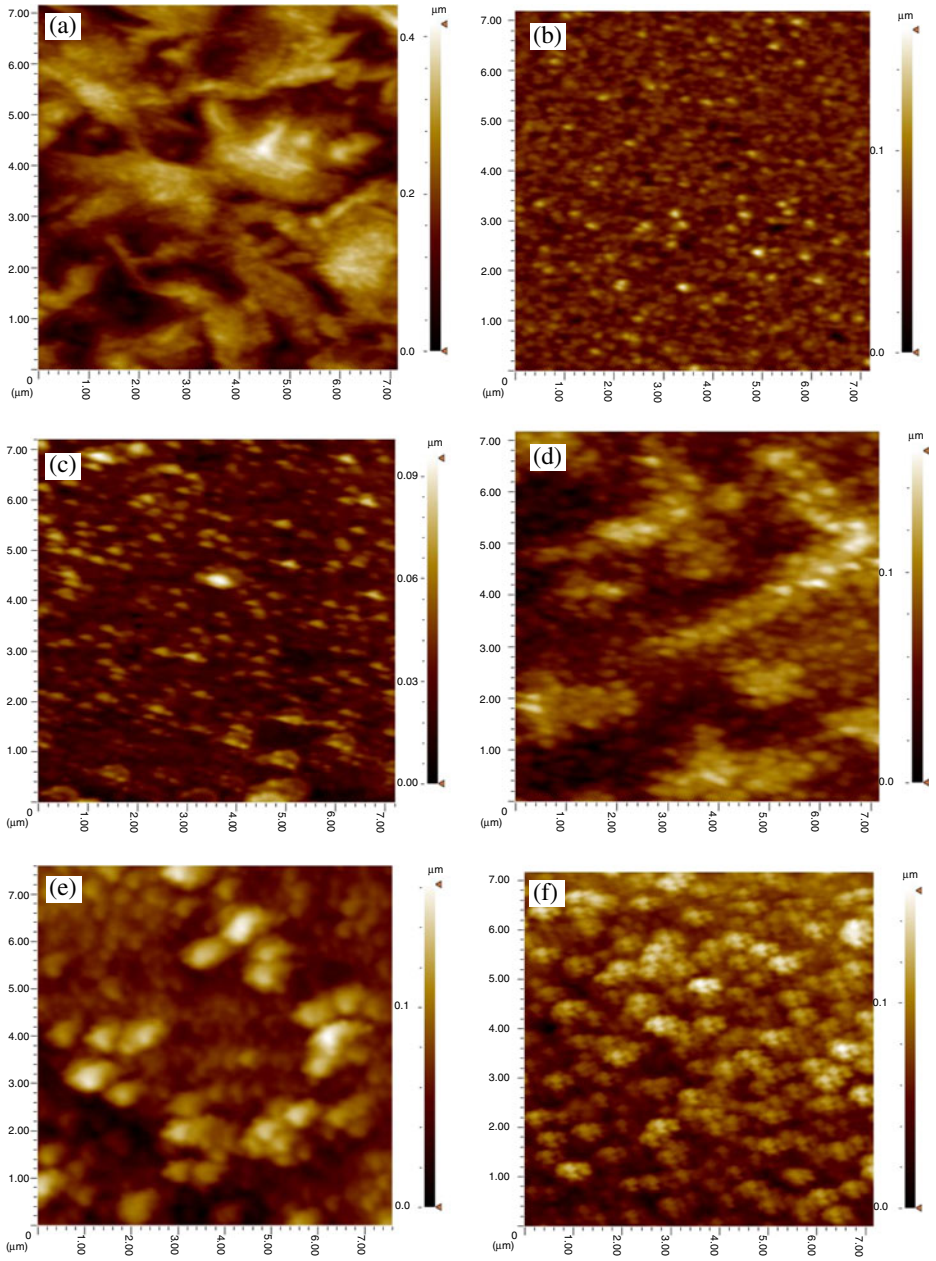

Figure 1. The AFM surface 2D images of FTO films as a function of F-doping concentrations: (**a**) 10 wt.%, (**b**) 15 wt.%, (**c**) 20 wt.%, (**d**) 25 wt.%, (**e**) 30 wt.%, (**f**) 35 wt.%.

Table 1. Values of the roughness parameter RMS, T_{avg}, the dislocation density (δ), the size of the crystallite (D) and figure-of-merit (ϕ) for FTO thin films with different doping concentrations.

Sample	D (nm)	δ ($\times 10^{15}$ lines/m^2)	RMS (nm)	T_{avg} (%) (at 700 nm)	ϕ ($\times 10^{-4}\ \Omega^{-1}$)
10 wt.% F	24.29	1.695	202	74.7	95
15 wt.% F	33.22	0.906	64	82.9	196
20 wt.% F	17.45	3.284	30	89.7	204
25 wt.% F	30.56	1.071	71	91.8	68
30 wt.% F	22.73	1.936	76	80.8	14
35 wt.% F	26.49	1.425	75	72.3	26

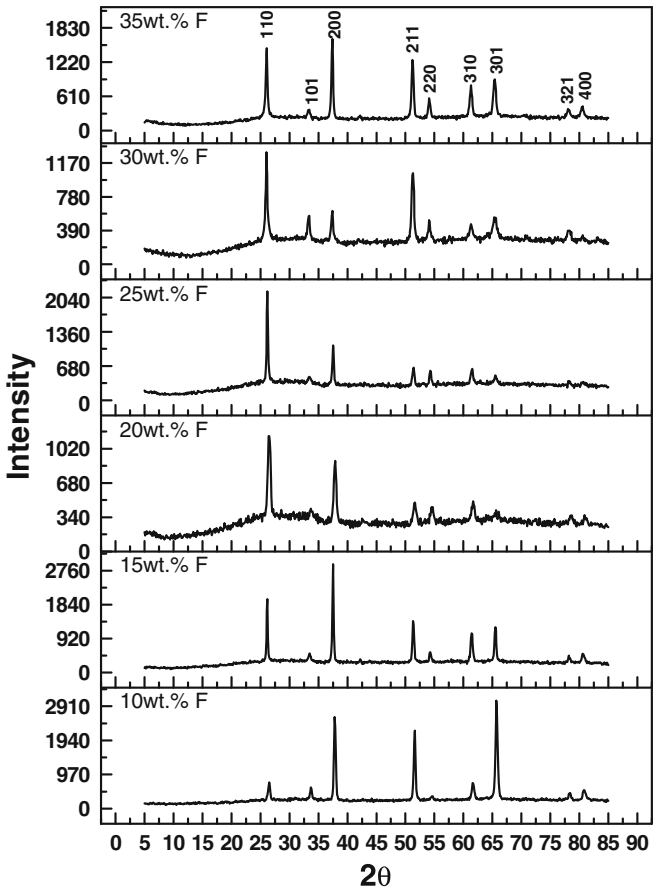

Figure 2. XRD spectra of the FTO films deposited on glass at different concentrations.

and (4 0 0) have also been detected but with substantially lower intensities at the higher doping concentration, which means the crystal growth is enhanced and the grain size is increased.

For films with 10 and 15 wt.% fluorine doping concentrations, the preferential orientation is (2 0 0) and for films with 20, 25 and 30 wt.% fluorine concentrations, the preferential orientation is (1 1 0). For films with 35 wt.% fluorine doping concentration, the most preferred orientation is (2 0 0) (figure 2). The preferred growth is always favoured by a high substrate temperature (fixed at 440°C) and a specific interaction of the nucleus with the substrate surface. The preferred orientation of a crystal plane depends on the surface energy of interaction, i.e., the orientation of the plane with lower surface energy of interaction is favoured [2]. In the present case, the (2 0 0) plane has been observed to have the minimum surface energy of interaction due to high substrate

Table 2. Structural parameters of FTO thin films with different doping concentrations.

Sample	(*h k l*)	d_{st} (Å)	d_{obs} (Å)	*a* (Å)	*c* (Å)
10 wt.% F	1 1 0	3.3470	3.3610	4.7532	3.2032
	2 0 0	2.3690	2.3766		
	2 1 1	1.7641	1.7699		
	3 0 1	1.4155	1.4199		
15 wt.% F	1 1 0	3.3470	3.4031	4.8127	3.2147
	2 0 0	2.3690	2.3957		
	2 1 1	1.7641	1.7785		
	3 0 1	1.4155	1.4237		
20 wt.% F	1 1 0	3.3953	3.3632	4.7563	3.2042
	2 0 0	1.7795	2.3725		
	2 1 1	1.6854	1.7699		
	3 0 1	1.4155	1.4215		
25 wt.% F	1 1 0	3.3470	3.4001	4.8085	3.2261
	2 0 0	2.3690	2.3948		
	2 1 1	1.7641	1.7776		
	3 0 1	1.4155	1.4235		
30 wt.% F	1 1 0	3.3470	3.4217	4.8390	3.2248
	2 0 0	2.3690	2.4038		
	2 1 1	1.7641	1.7800		
	3 0 1	1.4155	1.4273		
35 wt.% F	1 1 0	3.3470	3.4147	4.8291	3.2260
	2 0 0	2.3690	2.4032		
	2 1 1	1.7641	1.7820		
	3 0 1	1.4155	1.4259		

Standard JCPDS Card No: 41–1445; $a = 4.738$, $c = 3.187$

temperature of 440°C. Further, the intensity of the (2 0 0) peak increased fluorine doping concentration initially, but the intensity of the (1 1 0) peak decreased for increasing in F doping [1]. In addition to these issues, it has been reported that the preferred orientation depends on source of the compounds, solvent and growth parameters such as solution concentration, solution feed rate, deposition temperature and spraying gas pressure [26,36]. It was observed that the preferential orientations of crystal growth are strongly dependent on their concentration.

The thicknesses of SnO_2 films doped with 10, 15, 20, 25, 30 and 35 wt.% F were measured to be 271–1521 nm by conventional mass method [37] and were confirmed by the Swanepoel method using Standard formula [38]. The refractive indexes of films were seen to change from 1.65 to 1.6572. The grain sizes of SnO_2:F films deposited with different doping levels were calculated using Scherrer's formula [4,20,26,31], $D = 0.9\lambda/(\beta \cos\theta)$, where D is the size of the crystallite, β is the broadening of diffraction line measured at half its maximum intensity in radians and λ is the wavelength of X-rays ($\lambda = 1.5418$ Å). The calculated values of grain size and RMS are given in table 1. It may be seen that the grain size changes more slowly, before decreasing from 15 wt.% to 20 wt.%, then increasing up to 20 wt.%, then quickly decreasing up to 25 wt.% with increase in fluorine doping. This indicates that the grain size of the film depends on the concentration of the dopant. In this study, the obtained values for SnO_2:F thin films are in good agreement with the earlier report [39].

The lattice constants a and c, for the tetragonal phase structure is determined by the relation $(1/d^2) = \{[(h^2 + k^2)/a^2] + (l^2/c^2)\}$ where d is the interplaner distance and $(h\ k\ l)$ are Miller indices, respectively. The calculated lattice constants a and c are given in table 2. The lattice parameters a and c respectively are found to vary from 4.7532 to 4.8390 and 3.2032 and 3.2261 Å. The change in lattice constant for the spray-deposited thin film over the bulk clearly suggests that the film grains are strained, which may be due to the change in the nature and concentration of the native imperfections [40].

The growth mechanism involving dislocation is a matter of importance. Dislocations are imperfect in a crystal associated with the mis-registry of the lattice in one part of the crystal with respect to the other parts. Unlike vacancies and interstitial atoms, dislocations are insufficient to account for their existence in the observed dislocation densities [41–43]. The dislocation density (δ) is defined as the length of dislocation lines per unit volume, since δ is the measure of the amount of defects in a crystal. In our case, dislocation density (δ) was determined using the relation $\delta = 1/D^2$ where D is the size of the crystallite [40,43–45]. For SnO_2:F thin films these values are given in table 1 and the structural parameters are summarized in table 2.

3.2 *Electrical properties*

The electrical properties were investigated by Hall measurements in Van der Pauw configuration at room temperature. The negative sign of Hall coefficient confirmed the n-type conductivity of the films. Figure 3 shows resistivity (ρ), mobility (μ) and carrier concentration (n) of FTO films as a function of the doping levels. The results are also given in table 3. The values of μ, n and ρ are obtained from the combined measurements of resistivity and Hall coefficient. As seen in table 3, there is a decrease in the resistivity

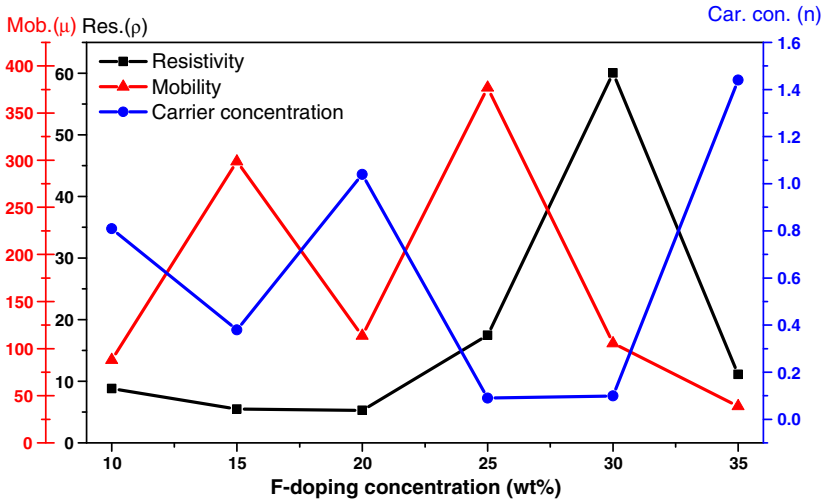

Figure 3. Resistivity, mobility and carrier concentration of FTO films as a function of F-doping concentration.

with the doping levels. It may be seen that resistivity decreases with increasing fluorine doping. As the doping level is increased from 10 wt.% to 20 wt.%, the resistivity (ρ) is decreased and then again increased. Hall mobility (μ) and carrier concentration (n) are also measured and the results are included in the same figure.

The sheet resistance (R_{sh}) of the films deposited on an optical glass substrate varied from 82.92 to 5.69 Ω/cm^2. Sheet resistance (R_{sh}) is a useful parameter for comparing thin films, particularly, those of the same material deposited under similar conditions [30]. The variation of sheet resistance and resistivity of SnO_2:F films with doping level are shown figure 4. For 20 wt.% F, both R_{sh} and ρ are found low. It is observed that the value of $\rho = 5.29 \times 10^{-4}$ ohm·cm is minimum for 20 wt.% F doping, indicating this to be the optimum concentration for possible applications. It is well known from many

Table 3. Electrical parameters (thickness (t), sheet resistance (R_s), electrical resistivity (ρ), electron mobility (μ), free electron concentration (n)) of FTO thin films with different doping concentrations.

Sample	t (nm)	R_s (Ω/cm^2)	ρ ($\times 10^{-4}$ Ω cm)	μ (cm^2/ V·s)	n ($\times 10^{20}$ cm^{-3})
10 wt.% F	271	5.69	8.79	87.87	0.809
15 wt.% F	312	7.81	5.49	298.76	0.38
20 wt.% F	692	16.52	5.29	113.52	1.04
25 wt.% F	699	62.22	17.48	377.02	0.09
30 wt.% F	743	82.92	60.03	105.52	0.099
35 wt.% F	1521	14.97	11.12	38.97	1.44

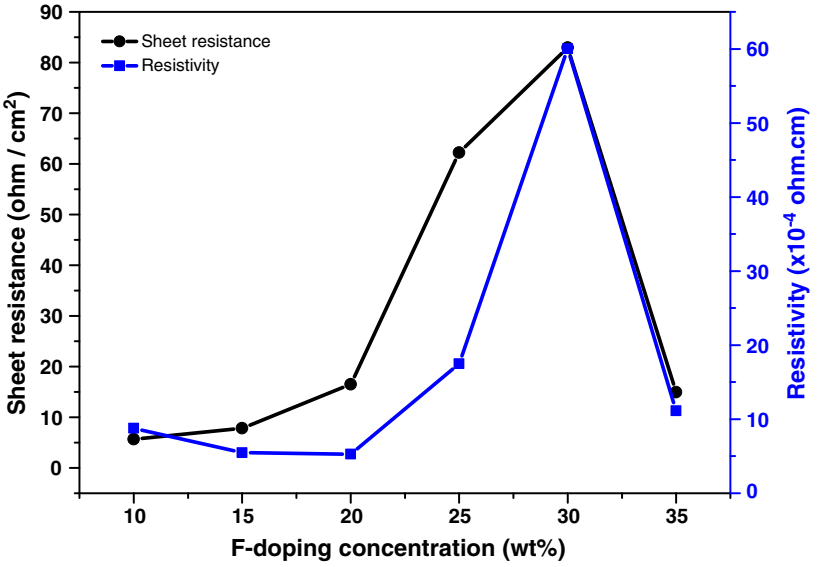

Figure 4. Variation of sheet resistance and resistivity of SnO_2:F films with different fluorine concentrations.

previous studies that the doping levels govern the stoichiometric variation of SnO_2 film. With increasing doping levels, the film becomes nonstoichiometric, which indicates that the surface mobility of the sputtered ions at the sample surface is enhanced with doping and thus the grain size becomes larger. This results in carrier scattering due to reduced grain boundaries and enhanced mobility. Also, the electrical properties of FTO films were enhanced with doping levels. This is consistent with the other studies [13].

3.3 *Optical properties*

Figure 5 shows the variation of transmittance (T) with respect to the wavelength of FTO thin films with different flourine doping levels. The maximum transmittance is 92% and 90% (700 nm), respectively for 25 wt.% F and 20 wt.% F concentration (table 1). The visible transmittance attained for the doped film in this study is higher than the values reported for 20 wt.% F-doped tin oxide films. The increase in transmittance is attributed to both the well-crystallized film and the pinhole free surface [30].

The thickness of the film is calculated using the following relation [4,47]:

$$t = \left(2\left[n(\lambda_1)/\lambda_1 - n(\lambda_2)/\lambda_2\right]\right)^{-1},$$

where $n(\lambda_1)$ and $n(\lambda_2)$ are the refractive indexes at the two adjacent maxima (or minima) at λ_1 and λ_2.

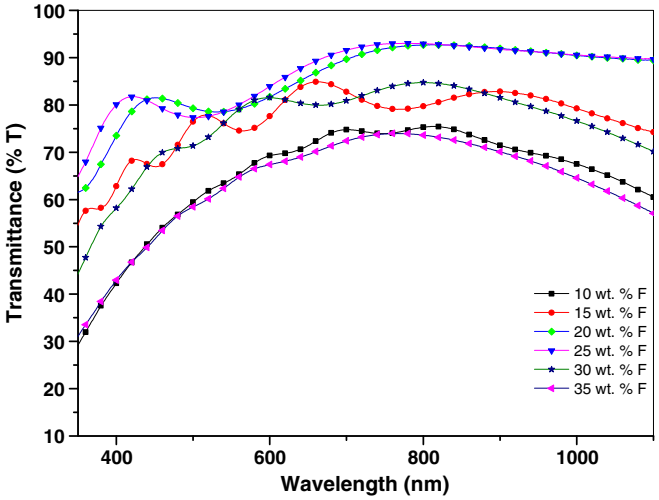

Figure 5. Optical transmission spectra of FTO thin films as a function of F-doping concentration.

The optical constants such as refractive index n and extinction coefficient $C(\lambda)$ are determined from a transmittance spectrum (figure 6) using envelope method. The refractive index can be calculated from the following equations:

$$n_{\text{film}} = 1/2([8n_{\text{sub}}C(\lambda) + (n_{\text{sub}} + 1)^2]^{1/2} + [8n_{\text{sub}}C(\lambda) + (n_{\text{sub}} - 1)^2]^{1/2})$$
$$C(\lambda) = [T^+(\lambda) - T^-(\lambda)]/[2T^+(\lambda) \cdot T^-(\lambda)],$$

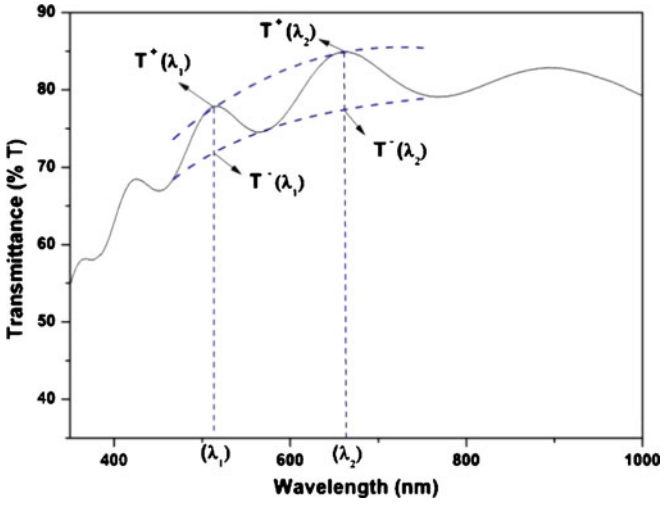

Figure 6. Transmission curve of interference envelope functions $T^+(\lambda)$ and $T^-(\lambda)$.

where n_{film} is the refractive index of the film at λ, n_{sub} is the refractive index of the substrate, $T^{+}(\lambda)$ is the maximum transmittance and $T^{-}(\lambda)$ is the minimum transmittance in the λ values.

To determine these values, similar calculations have been done for ZnO thin films by Bazavan *et al* [46], by Moholkar *et al* [39] and by Gümüş *et al* [47]. For a sample the interference envelopes passing through the extreme points in the spectrum are shown in figure 6.

The variation of thickness of the deposited films is shown in figure 7 and table 3 from which, it is seen that as the concentrations of F in spraying solution increases, film thickness increases. Moholkar *et al* [39] have explained this as follows: as the concentration increases, thickness increases continuously due to the relative increase in Sn^{2+} and F^{-} ions in the solution.

The figure-of-merit is an important parameter for evaluating FTO thin films for use in solar cells [31]. To compare the performance of various transparent conductors the most widely used figure-of-merit as defined by Haacke is $\Phi_{\text{M}} = T^{10}/R_{\text{sh}}$ [3,26,31,36], where T is the transmittance at 700 nm and R_{sh} is the sheet resistance. This formula gives more weight to the transparency and thus is better adapted to solar cell technology [31]. It is clear that figure-of-merit depends on the sheet resistance. The calculated figure-of-merit values are given in table 1. It was found (table 1) that the value obtained for the films doped with 20 wt.% F is the highest in the present study ($204 \times 10^{-4}\ \Omega^{-1}$) because the formation of good quality film in terms of conductivity and transmittance is possible only at this deposition concentration. The obtained values are in good agreement with the earlier reports [31,36,45,48].

Figure 8 shows the plot of sheet resistance and figure-of-merit as a function of fluorine doping concentration. R_{sh} increases with increasing F concentration and thereafter it decreases. The figure-of-merit increases with increasing F concentration, becomes a maximum of $204 \times 10^{-4}\ \Omega^{-1}$ for 20 wt.% F and thereafter it decreases (figure 8).

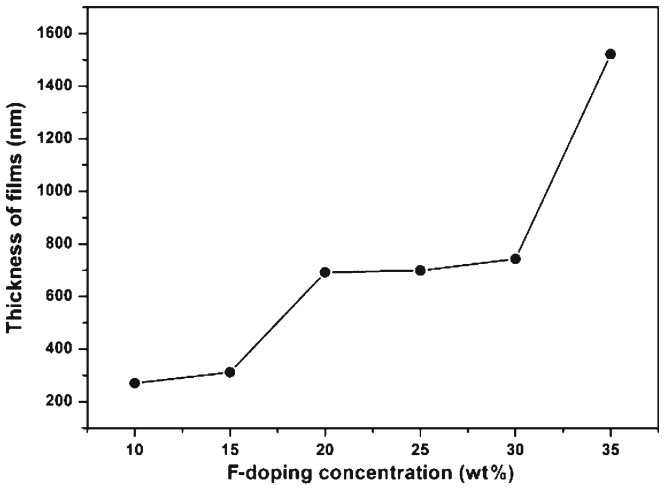

Figure 7. Variation of the film thickness of FTO thin films as a function of F-doping concentration.

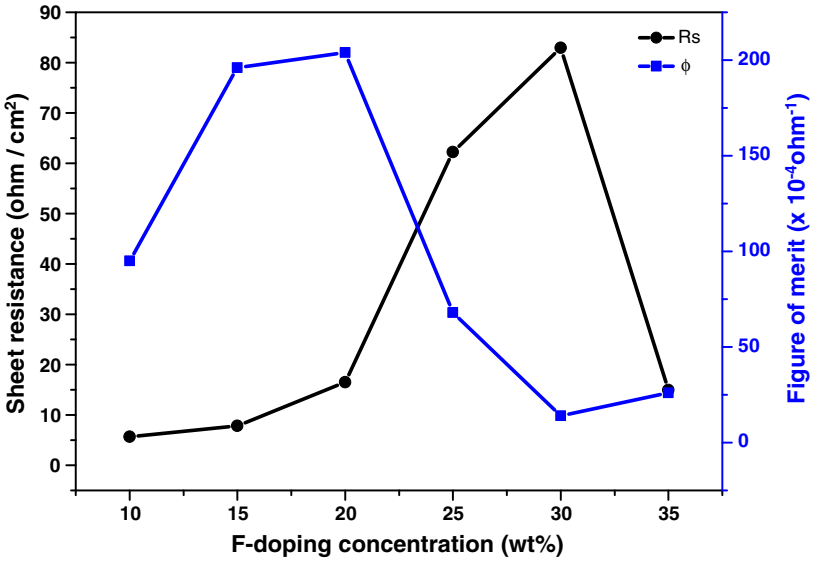

Figure 8. Plot of sheet resistance and figure-of-merit as a function of F-doping concentration.

4. Conclusions

Polycrystalline thin films of SnO_2 with different ([F]/[Sn] ratios) fluorine doping concentrations were prepared using a home-made spray pyrolysis apparatus at substrate temperature 440°C onto optical glasses. The effects of doping levels on the structural, electrical and optical properties of SnO_2:F were experimentally investigated. X-ray diffraction studies revealed that the material in the thin form is polycrystalline with tetragonal structure. The Hall measurements showed that the conductivity of the films is of n-type. The electrical conductivity characteristics, atomic force microscope (AFM) images, UV–vis spectra and X-ray diffraction patterns confirmed that the crystallinity is effected by doping levels. The FTO films are very smooth. X-ray diffraction pattern revealed the presence of cassiterite structure with (1 1 0), (2 0 0), (2 1 1) and (3 0 1) preferential orientations for FTO films. The lowest sheet resistance (R_{sh}) for the SnO_2:F films was 5.69 Ω/cm^2. The average visible transmittance (T) at 700 nm of the deposited films was 91.8%. The value of the figure-of-merit (ϕ) in the FTO films at 700 nm was 204 $\times$ 10^{-4} Ω^{-1}. All the films were degenerate with carrier concentrations (n) in the range of 0.09 $\times$ 10^{20}–1.44 $\times$ 10^{20} cm^{-3}. The resistivity (ρ) and mobility (μ) of the samples were of the order of 5.29 $\times$ 10^{-4}–60.03 $\times$ 10^{-4} Ω·cm and 38.97–377.02 $cm^2/V{\cdot}s$, respectively. The grain size (D) was also found in the range of 17.45–33.22 nm. The obtained results suggest that the deposited films can be used as transparent electrodes in solar cells applications.

Similar studies were done previously by many researchers. In this paper, we emphasize the similarities and differences between the results obtained by us and by other researchers. The resistivity attained (5.29 $\times$ 10^{-4} Ω·cm) for the doped film (prepared

at 440°C) in this study is lower than the values reported for 20 wt.% F-doped tin oxide films prepared from aqueous solution of $SnCl_2{\cdot}2H_2O$ precursor [5,30]. The highest transmittance of about 91.8% at 700 nm has been observed. The transmission attained in this study is greater than the values reported for fluorine-doped tin oxide films [26,30]. Irrespective of differences and similarities, most important results were obtained from the study.

References

[1] D Miao, Q Zhaoa, S Wua, Z Wange, X Zihanga and X Zhaoa, *J. Non-Cryst. Solids* **356**, 2557 (2010)
[2] G J Exarhos and X D Zhou, *Thin Solid Films* **515**, 7025 (2007)
[3] E Elengovan and K Ramamurthi, *J. Optoelectron. Adv. Mater.* **5**/**1**, 45 (2003)
[4] A A Yadav, E U Masumdar, A V Moholkar, M Neumann-Spallart, K Y Rajpure and C H Bhosale, *J. Alloys and Compounds* **448**, 350 (2009)
[5] B Thangaraju, *Thin Solid Films* **402**, 71 (2002)
[6] A Goetzberger and C Hebling, *Sol. Energy Mater. Sol. Cells* **62**, 1 (2000)
[7] G Frank, E Kaur and H Kostlin, *Sol. Energy Mater.* **8**, 387 (1983)
[8] S Chen, *Thin Solid Films* **77**, 127 (1981)
[9] W Y Chung, C H Shim, S D Choi and D D Lee, *Sens. Act.* **B20**, 139 (1994)
[10] J R Brown, P W Haycock, L M Smith, A C Jones and E W Williams, *Sens. Act.* **B63**, 109 (2000)
[11] P Nelli, G Faglia, G Sberveglieri, E Cerede, G Gabetta, A Dieguez and J R Morante, *Thin Solid Films* **371**, 249 (2000)
[12] I Stambolova, K Konstantinov and T Tsacheva, *Mater. Chem. Phys.* **63**, 177 (2000)
[13] S U Lee, W S Choi and B Hong, *Phys. Scr.* **T129**, 312 (2007)
[14] E Elangovan, S A Shivashankar and K Ramamurthi, *J. Crystal Growth* **276**, 215 (2005)
[15] P S Patil, *Mater. Chem. Phys.* **59**, 185 (1999)
[16] M Ruske, G Brauer and J Szczrbowski, *Thin Solid Films* **351**, 146 (1999)
[17] Q Zhao, S Wu and D Miao, *Adv. Mater. Res.* **150–151**, 1043 (2011)
[18] D Belanger, J P Dotelet, B A Lombos and J I Dickson, *J. Electrochem. Soc.* **398**, 1321 (1985)
[19] A C Arias, L S Roman, T Kugler, R Toniola, M S Meruvia and I A Hummelgen, *Thin Solid Films* **371**, 201 (2000)
[20] P S Shewale, S I Patil and M D Uplane, *Semicond. Sci. Technol.* **25**, 115008 (2010)
[21] O K Varghese and L K Malhotra, *J. Appl. Phys.* **87**, 7457 (2000)
[22] M K Karanjai and D D Gupta, *J. Phys. D: Appl. Phys.* **21**, 356 (1988)
[23] G Gordillo, L C Moreno, W de la Cruz and P Theran, *Thin Solid Films* **252**, 61 (1994)
[24] A Malik, A Seco, E Fortunato and R Martin, *J. Non-Cryst. Solids* **1092**, 227 (1998)
[25] B Zhang, Y Tian, J C Zhang and W Cai, *J. Mater Sci.* **46**, 1884 (2011)
[26] A V Moholkara, S M Pawara, K Y Rajpureb, S N Almaric, P S Patilb and C H Bhosale, *Solar Energy Mater. Solar Cells* **92**, 1439 (2008)
[27] Q Chen, Y Qian, Z Chen, G Zhou and Y Zhang, *Thin Solid Films* **264**, 25 (1995)
[28] A Smith, J M Laurent, D S Smith, J P Bonnet and R R Clemente, *Thin Solid Films* **266**, 20 (1995)
[29] K Omura, P Veluchamy and M Murozono, *J. Elecktrochem. Soc.* **146**, 2113 (1999)
[30] A V Moholkar, S M Pawara, K Y Rajpure, C H Bhosale and J H Kim, *Appl. Surface Sci.* **255**, 9358 (2009)
[31] N Menarian, S M Rozati, E Elemurugu and E Fortunato, *Phys. Status Solidi* **C79**, 2277 (2010)

[32] E Elengovan and K Ramamurthi, *Appl. Surface Sci.* **249**, 183 (2005)
[33] S J Ikhmayies and R N Ahmad-Bitar, *Mater. Sci. Semicond. Process* **12(3)**, 122 (2009)
[34] T M Mohammad, *Sol. Energy Mater.* **20(4)**, 297 (1990)
[35] E A Rakhshani, Y Makdisi and A H Ramazaniyan, *J. Appl. Phys.* **83**, 1049 (1998)
[36] A V Moholkar, S M Pawara, K Y Rajpureb and C H Bhosale, *Mater. Lett.* **61**, 3030 (2007)
[37] B Thangaraju, *Thin Solid Films* **402**, 71 (2002)
[38] J Sanchez-Gonzalez, A Diaza-Parralejo, A L Ortiz, and F Guiberteau, *Appl. Surface Sci.* **252**, 6013 (2006)
[39] A V Moholkar, S M Pawar, Y K Rajpure and C H Bhosale, *J. Alloys and Compounds* **455**, 440 (2008)
[40] C M Shen, X G Zhang and H L Li, *Appl. Surf. Sci.* **240**, 34 (2005)
[41] R R Kasar, N G Deshpande, Y G Gudage, J C Vyas and R Sharma, *Physica* **B403**, 3724 (2008)
[42] A Beltron and J Andres, *Appl. Phys. Lett.* **83**, 635 (2003)
[43] M Bedir, M Öztaž, O F Bakkaloglu and R Ormanel, *Eur. Phys. J.* **B45**, 465 (2005)
[44] M Kojima, H Kato and M Gatto, *Phil. Mag.* **B68**, 215 (1993)
[45] M Dhanam, R Balsundharprabhu, S Jayakumar, P Gopalkrishnan and M D Kannan, *Phys. Status Solidi* **A19**, 149 (2002)
[46] R Bazavan, L Ion, G Socol, I Enculescu, D Bazavan, C Tazlaoanu, A Lõrinczi, I N Mihailescu, M Popescu and S Antohe, *J. Optoelectron. Adv. Mater.* **11(4)**, 425 (2009)
[47] C Gümüž, O M Ozkendir, H Kavak and Y Ufuktepe, *J. Optoelectron. Adv. Mater.* **8/1**, 299 (2006)
[48] K S Ramaiah and V S Raja, *Appl. Surf. Sci.* **253**, 1451 (2006)